Accelerator Adsorption onto Carbon Nanotubes Surface Affects the Vulcanization Process of Styrene–Butadiene Rubber Composites

A. De Falco,[1] A. J. Marzocca,[1] M. A. Corcuera,[2] A. Eceiza,[2] I. Mondragon,[2] G. H. Rubiolo,[1,3,4] S. Goyanes[1,4]

[1]*Laboratorio de Polímeros y Materiales Compuestos, FCEyN, Univ. Nac. de Buenos Aires. Pabellón 1 Ciudad Universitaria, Buenos Aires 1424, Argentina*
[2]*'Materials + Technologies' Group, Escuela Politécnica, Dpto. Ingeniería Química y M. Ambiente, Universidad País Vasco, Donostia-San Sebastián, Spain*
[3]*Unidad de Actividad Materiales, Comisión Nacional de Energía Atómica (CNEA – CAC), Avda Gral Paz 1499, B1650KNA, San Martín Argentina*
[4]*CONICET, Consejo Nacional de Investigaciones Científicas y Tecnológicas, Argentina*

Received 18 March 2008; accepted 13 February 2009
DOI 10.1002/app.30261
Published online 1 May 2009 in Wiley InterScience (www.interscience.wiley.com).

ABSTRACT: The multiwalled carbon nanotubes (MWCNT) filled styrene–butadiene rubber (SBR) composites were prepared by incorporating MWCNT in a SBR/toluene solution and subsequently evaporating the solvent. These composites have shown a significant improvement in Young's modulus and tensile strength with respect to SBR gum without sacrificing high elongation at break. However, this improvement is less than expected at the higher filler content. Then, the influence of low concentrations of MWCNT on the vulcanization process of the SBR composites was studied by means of rheometer torque curves, swelling measurements, differential scanning calorimeter (DSC) analysis, and Fourier transform infrared (FTIR) spectroscopy. Also, their thermal degradation was studied by thermogravimetric analysis (TGA). It has been noticed that MWCNT affects the cure kinetics of SBR gum matrix reducing all parameters, i.e., the total heat rate and order of the reaction, scorch delay, maximum torque, and cross-link density. This effect increases as MWCNT content does, and it was attributed to the adsorption of the accelerator employed in the vulcanization (*N*-tert-butyl-benzothiazole-2-sulfenamide) onto the MWCNT surface. J Appl Polym Sci 113: 2851–2857, 2009

Key words: carbon nanotubes; elastomers; vulcanization; nanocomposites; nanotechnology

INTRODUCTION

Composites based on styrene–butadiene rubber are used frequently in technical applications because of their good mechanical properties, especially in the tire manufacture industry. Carbon black and silica are perhaps the reinforcing particles most widely used in elastomers.

In recent years, there has been a high interest in the application of carbon nanotubes (CNT) as reinforcement in elastomer matrix composites.[1–3] This is because of their excellent mechanical, thermal, and electrical properties.[4] Besides, carbon nanotubes have a high aspect ratio, which makes them an ideal filler when it is necessary to transmit stresses between matrix and filler.

Recently, two methods have been reported to prepare multiwalled carbon nanotubes (MWCNT)-filled styrene–butadiene rubber (SBR) composites. The first one obtains the composites by vulcanization of a powder prepared by spray drying of the suspension of MWCNT in SBR latex.[5,6] In the second, the authors have vulcanized a gum matrix composite prepared by incorporating MWCNT in a SBR/toluene solution and subsequently evaporating the solvent[7]; this method was later used in reference.[8] Both methods allow improving dispersion of MWCNT in the rubber and mechanical properties compared with the results obtained by the traditional mechanical mixing process. However, for both the methods, the curing time of the composites filled with MWCNT is longer than that filled with carbon black, that is, MWCNT seems to decelerate the vulcanization of SBR composites.

The cure reactions of elastomeric composites based on sulphur and accelerator are complex because of the occurrence of many reactive processes simultaneously. Among the available accelerators, there are three groups, which are widely known.[9,10] First, aniline and other amines, which are not used

Correspondence to: S. Goyanes (goyanes@df.uba.ar).

TABLE I
Matrix Formulation

Ingredient	Quantity (phr)
SBR-1502	100
Zinc oxide	5.0
Stearic acid	2.0
Antioxidant	1.2
Sulphur	2.0
TBBS	1.0

phr = Per hundred rubber.

today because of their toxicity. Second, dithiocarbamates, which albeit having the best crosslinking rate, have almost no scorch resistance (the time required, at a certain temperature, for the onset of the crosslink formation). Finally, benzothiazoles and its derivatives are most extensively used today because of their excellent scorch properties.[10,11] The accelerator is thought to react with sulphur to produce monomeric polysulfides, which, in turn, interacts with the rubber to form polymeric polysulfides. Besides this accelerant, zinc oxide and a fatty (stearic) acid are also used to activate the reaction. The zinc oxide forms a salt with the acid, which increases the effect of the accelerator. It is customary to use this fatty acid in excess.

The main differences in the vulcanizing reagent recipe for SBR in the previous works were the sulfur/accelerator ratio[5–7] and the derivatives of benzothiazoles used as accelerator [benzothialzyl disulfide (DM)[5,6]; *n-t*-butyl-2-benzothiazole sulfenamide (TBBS)[7]].

In this article, the effects of small addition of MWCNT on SBR vulcanization reaction with sulphur/TBBS cure system were studied by means of rheometer torque curves, differential scanning calorimeter (DSC) analysis, and Fourier transform infrared (FTIR) spectroscopy. The effects on thermal degradation were also studied by thermogravimetric analysis (TGA).

EXPERIMENTAL

The elastomer employed as matrix was styrene–butadiene rubber SBR-1502, with an average molecular weight of M_n = 91,350 g/mol, as determined by gel permeation chromatography, and a density ρ_{SBR} = 0.935 g/cm^3.

The MWCNT from Nanocyl (3100), after ultrasonic dispersion in ethanol,[12] were used as reinforcement. The composites were prepared according to our previous work.[7] The curing system based on sulphur and TBBS as accelerator was used as shown in the formulation of Table I. The curatives and the nanotubes were incorporated to dissolution of SBR in toluene, 25 mL/g, and then the ultrasonic dispersion was carried out on the mixture for 5 h. Finally, the mixture was poured over Petri capsules to let the toluene evaporate for 3 days.

Three composites were prepared with MWCNT content of 0 wt % (gum matrix); 0.33 and 0.66 wt %, respectively. The temperature of cure was evaluated by differential scanning calorimetry performed in a DSC-7 Perkin Elmer, at 10°C/min, in nitrogen atmosphere with a flow of 20 cm^3/min. The cure characteristics of the different compounds were measured with a Rheometric Scientific RDA ARES using a 1-mm gap between parallel plates.

Infrared spectra of the cured matrix and compounds were recorded on a Genesis II FTIR spectrometer using the attenuated total reflectance (ATR) accessory. The spectra were measured at a resolution of 2 cm^{-1}, averaging more than 32 scans.

Thermal degradation of the cured samples was investigated using a TGA 92-12 Setaram thermogravimetric apparatus.

The morphologies of CNT and the cryogenic fractured surfaces of the vulcanized rubber composites were observed using a DSM 982 GEMINI field emission scanning electron microscope (FE-SEM).

Crosslink densities of the rubber compounds were measured by swelling method. Cured discs of 17 mm diameter and 1 mm thickness were prepared from the uncured matrix and compounds. Organic additives in the samples were removed by standing 24 h in pyridine and extracting for 16 h in acetone. After extraction, the samples were dried at room temperature until constant weight was obtained in the samples.

The organic material-extracted samples were immersed completely in toluene and swelling equilibrium occurred approximately in 48 h. Then, the swollen samples were surface dried with filter paper and quickly weighted. The weights of both the organic material-extracted and swollen samples were

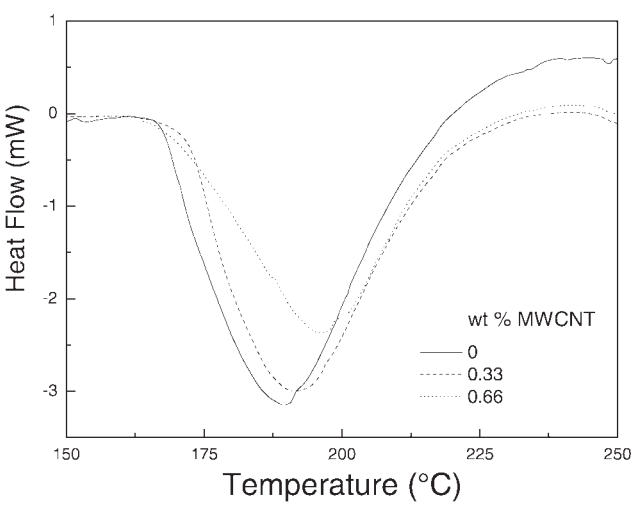

Figure 1 Effect of MWCNT on curing of rubber composites by DSC analysis.

TABLE II
Total Heat of Reaction and Maximum Exothermal Peak Temperature

Material	ΔH (J/g)	T_p (°C)
Matrix	29 ± 1.0	190
0.33 wt % MWCNT	26 ± 0.5	192
0.66 wt % MWCNT	23 ± 0.5	196

measured to 0.0001 g. The volume fraction of rubber, V_{2m}, was obtained using the following equation:

$$V_{2m} = \frac{W_d/\rho}{W_d/\rho + (W_s - W_d)/\rho_s}$$

where W_d and ρ are the weight and density of the sample after drying, W_s the weight of the swollen sample, and ρ_s the density of the solvent. The values of V_{2m} so obtained were converted into V^0_{2m} (the value V_{2m} would have in the absence of the carbon nanotubes) according to the Porter relationship[13]

$$V^0_{2m}/V_{2m} = 0.56\exp(-z) + 0.44$$

where z is the weight concentration of carbon black which surface area is equivalent to that of the weight concentration of the carbon nanotubes, z_{cnt}, actually loaded in the samples. The z parameter was calculated as

$$z = \frac{3}{4}\frac{\rho_{cb} \times r_{cb}}{\rho_{cnt} \times r_{cnt}} z_{cnt}$$

where (ρ_{cb}, r_{cb}) and (ρ_{cnt}, r_{cnt}) are the (density, radius) of carbon black, taken as a spherical particle, and carbon nanotubes, respectively.

The molecular weight of the network chain between chemical crosslinks for a phantom network, M_{cs}, was calculated by the Flory–Rehner relationship[14,15]

$$M_{cs} = \frac{-\rho\left(1 - \frac{2}{\varphi}\right) V_1 (V^0_{2m})^{1/3}}{\ln(1 - V^0_{2m}) + \chi (V^0_{2m})^2 + V^0_{2m}}$$

where φ is the functionality of the crosslinks, V_1 is the molar volume of solvent, and χ is the interaction parameter between the polymer and the swelling agent. The following values for these constants were used: $\rho_{cb} = 1.86$ g/cm^3; $r_{cb} = 5 \times 10^{-5}$ cm; $\rho_{cnt} = 1.82$ g/cm^3; $r_{cnt} = 1.5 \times 10^{-6}$ cm; $\varphi = 4$; $V_1 = 106.29$ mL/mol[16]; $\chi = 0.446$[17]; and $\rho_s = 0.8669$ g/cm^3.[16]

RESULTS AND DISCUSSION

The results of DSC tests are shown in Figure 1. The total heat of reaction (ΔH) and the maximum exothermal peak temperature (T_p) are reported in Table II. A decrease of the ΔH and a shift to higher T_p values is observed for both composites with respect to the matrix as the MWCNT contents increases. These results are in agreement with those reported by Zhou et al.[6] for high MWCNT content. It should be noted that the start of all three exothermic peaks is located at a temperature slightly above 155°C, then the vulcanization temperature was chosen at 155°C and the cure time was determined from the rheometric curves at that temperature.

Rheometric curves of torque versus time are shown in Figure 2. Some interesting facts can be observed. There is a decreasing scorch delay (induction time t_0) and the curing time at the inflection point is longer when the amount of nanotubes increases in the samples. Also, there is a higher value of maximum torque in the loaded composites. The maximum torque obtained for the composite with 0.33 wt % CNT is 14% higher than that of the matrix, whereas the maximum torque of the composite with 0.66 wt % is only 17% higher than that of the matrix. Other researchers[5,6,18] reported similar results in rheometric behavior in elastomers but with CNT content higher than 2 wt %.

To quantify the results of the cure reaction, the kinetic parameters were obtained from the normalized torque θ curves according to the isothermal cure model proposed by Kamal and Sourour[19]:

$$\theta = \{k_r(t - t_0)\}^n / \{1 + (k_r(t - t_0))^n\} \quad (1)$$

where the parameter θ is considered the state of the cure, k_r is the reaction rate, n the reaction order, and t_0 the induction time (scorch time).

The normalized torque curves were obtained as:

$$\theta = (\tau_t - \tau_l)/(\tau_h - \tau_l) \quad (2)$$

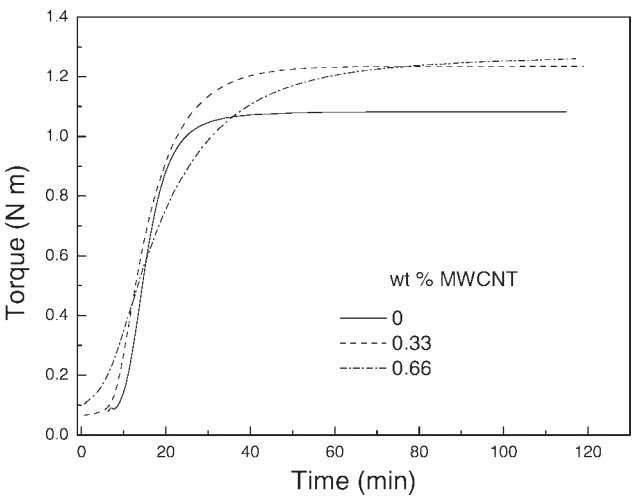

Figure 2 Effect of MWCNT on the vulcanization torque of the composites.

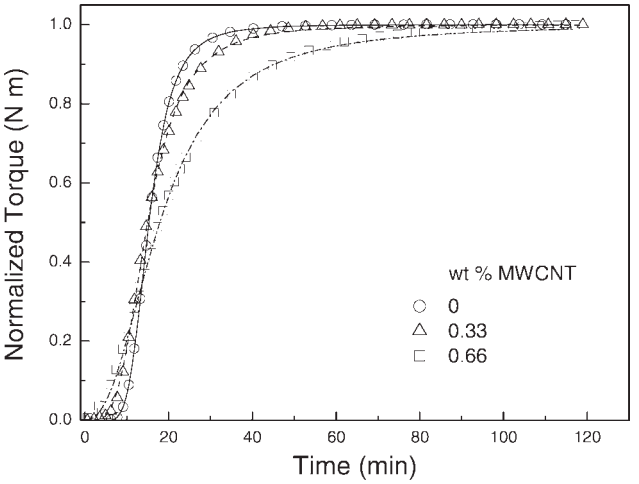

Figure 3 Curve fitting of Kamal–Sourour equation to normalized torque curves from the data in Figure 2.

where τ_t is the torque at time t, τ_l, and τ_h are the minimum and the maximum torque, respectively. This model was used successfully to analyze the vulcanization kinetics of SBR with the system TBBS and sulphur.[20,21]

The fitted curves are shown in Figure 3, and the parameters obtained are indicated in Table III. As expected, the parameters show that the presence of carbon nanotubes in the composite leads to a decrease in the reaction rate, as well as in the reaction order, and in the scorch time.

It is interesting to note that results of both tests, DSC and torque curves, agree in that the addition of carbon nanotubes generates a delaying effect not only in the formation of the crosslinked network (rheometric curves) but also in all reactions (DSC curves). It should be taken into account that DSC measures the heat from all the reactions, whereas the rheometric curves are affected only by the reactions that lead to elasticity.[22]

Figures 4 shows a micrograph of the MWCNT employed in the composite. It can be seen that they have an average diameter of 15 nm and, at least, an aspect ratio of 200, which agrees with the data given by the supplier.

Figure 5(a) shows a micrograph of the fractured surface of the composite containing 0.66 wt % MWCNT. The bright dots are the ends of carbon nanotubes. Clearly, carbon nanotubes are dispersed homogeneously in the rubbery matrix. A composite

TABLE III
Cure Reaction Kinetics Parameters

Material	k_r (10^{-2} min^{-1})	n	t_0 (min)
Matrix	9.52 ± 0.03	3.77 ± 0.01	4.83 ± 0.03
0.33 wt % MWCNT	7.58 ± 0.09	3.19 ± 0.03	1.80 ± 0.10
0.66wt % MWCNT	5.59 ± 0.06	2.37 ± 0.02	0

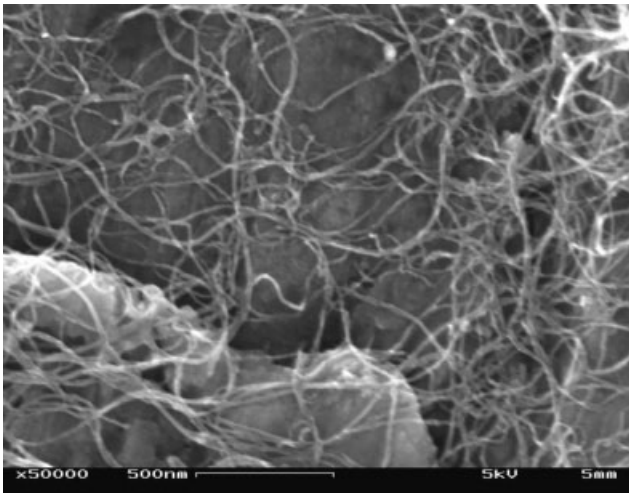

Figure 4 FE-SEM image of raw MWCNT.

micrograph with a higher resolution and lower length scale is shown in Figure 5(b). Closer examination of the nanotubes reveals an average diameter of

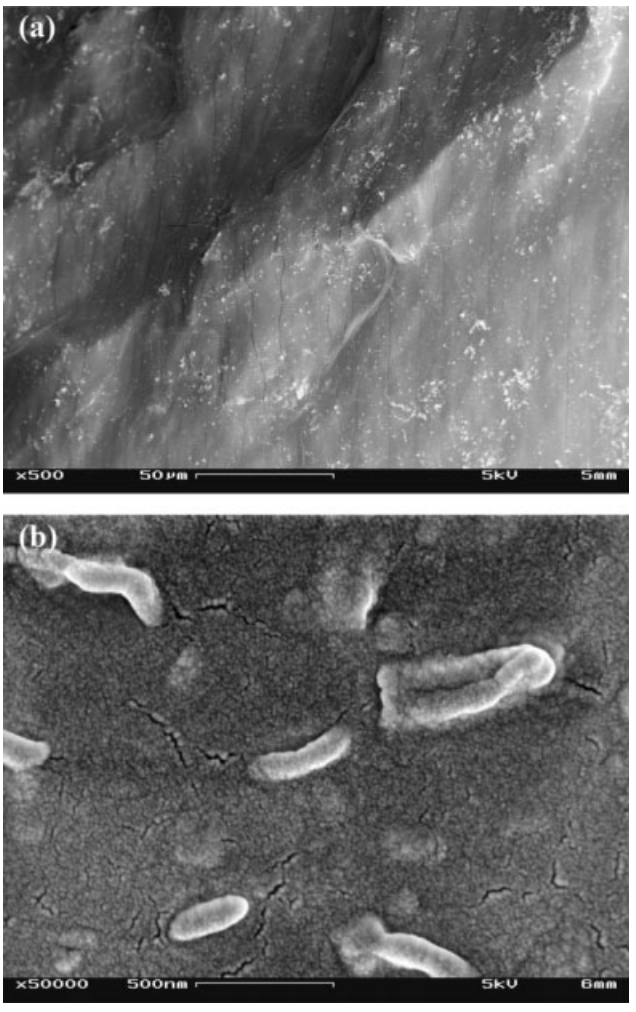

Figure 5 FE-SEM images of the fractured surface of SBR/MWCNT (0.66 wt %) composite.

133 nm, which suggests that a thick layer of SBR covers the CNT surface, indicating some degree of wetting and that there is a good phase adhesion of the polymer chains to the walls of the CNT.

To analyze the values of the maximum torque given in the rheometer curves, some consideration can be pointed out. As it is known, in the rheometer test, the torque is related to the shear modulus and then the following relation can be used

$$\frac{\tau_{comp}}{\tau_0} = \frac{G_{comp}}{G_0} \tag{3}$$

where (τ_0, G_0) and (τ_{comp}, G_{comp}) are the torque and the shear modulus of the matrix and the composite, respectively. Because of the thickness of the rheometer sample, given by the gap between parallel plates, the average length of nanotubes ($\approx$ 3 μm) and its low concentration in these composites, the nanotubes may be considered oriented randomly in three dimensions. An approximate inequation from eq. (3) can be obtained in this case:

$$\frac{\tau_{comp}}{\tau_0} = \frac{G_{comp}}{G_0} = \frac{E_{comp}\ (1 + 2\ \nu_0)}{E_0\ (1 + 2\ \nu_{comp})} \geq \frac{E_{comp}}{E_0} \tag{4}$$

where (ν_0, E_0) and (ν_{comp}, E_{comp}) are the Poisson and the Young's modulus of the matrix and the composite, respectively, and $\nu_{comp} \geq \nu_0$ is supposed. Now, given that the aspect ratio of the MWCNT can be known (estimated from Fig. 4, it is around 200), the right hand of inequation (4) can be estimated with the simplified model of Halpin-Tsai for low filler contents randomly aligned[1,23]:

$$E_L = E_0 \left(\frac{1 + 2fc}{1 - c}\right)$$
$$E_T = E_o \left(\frac{1 + 0.5c}{1 - c}\right)$$
$$E_{random} = \frac{1}{5}\ E_L + \frac{4}{5}\ E_T$$

where E_L is the modulus for a composite with perfectly parallel aligned filler, E_T is the modulus for a composite with perfectly perpendicular aligned filler, f is the aspect ratio of the filler, and c is the volume concentration of the filler. This estimation predicts a 14% increment for the composite with 0.33 wt % CNT and 28% for the composite with 0.66 wt % CNT while the experimental values are 14% and 17%, respectively. Because a good phase adhesion of the polymer chains to the walls of the CNT was shown [Fig.5(b)], the discrepancy between the experimental and theoretical values for the composite with 0.66 wt % CNT seems to come more than from a less crosslinked matrix that from a friction loss between matrix and MWCNT. This fact is confirmed by the crosslink density evaluated in each cured sample from swelling tests. Our experimental results of M_{cs} are shown in Table IV together with the crosslink density μ obtained by using[24]

$$\mu = \frac{\rho_{SBR}}{2}\left(\frac{1}{M_{cs}} - \frac{1}{M_n}\right)$$

TABLE IV
Values of Molecular Weight Between Chemical Crosslink, M_{cs}, and Crosslink Density, μ, Obtained From Swelling Measurements of All Samples Cured at 155 °C

Material	M_{cs} (10^3 g mol^{-1})	μ (10^{-6} mol cm^{-3})
Matriz	9.1 ± 0.2	46.5 ± 0.8
0.33 wt % MWCNT	9.00 ± 0.08	47.0 ± 0.5
0.66 wt % MWCNT	11.4 ± 0.1	36.1 ± 0.5

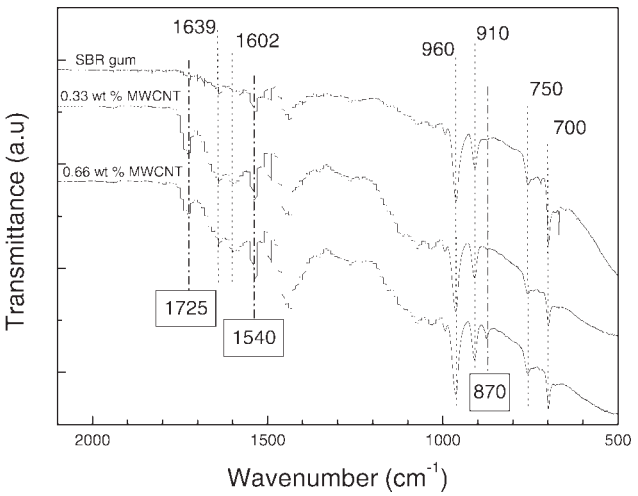

Figure 6 ATR-FTIR spectra for SBR/MWCNT composites containing different MWCNT contents.

Figure 6 shows the infrared (IR) spectra of SBR gum and SBR-MWCNTs composites. According to bibliography,[25–27] there are several bands that must be used in order to identify the components of the SBR vulcanized. Thus, two spectral regions are identified, one between 700 and 1000 cm^{-1} and the other around 1600 cm^{-1}.

The diagnostic bands, in the lower wavelength region, correspond to the out of plane bending vibrations of aromatic =C—H and C=C groups of polystyrene at 750 and 700 cm^{-1}, respectively, and the out of plane bending vibrations of =C—H of vinyl groups (990 and 910 cm^{-1}) and trans —CH=CH— at 960 cm^{-1} of butadiene.[25,26] All of them are clearly present in our samples with the exception of the band at 990 cm^{-1}, which is almost imperceptible.

In the middle wavelength region, the diagnostic bands are attributed to the carbon–carbon stretching vibration of the aromatic double bond at 1602 cm^{-1},

ascribed to the styrene content of the elastomer, and to the stretching vibration of the olefinic portion of the elastomer at 1639 cm^{-1}, ascribed to the butadiene.[27] These two bands appear more clearly in our composites spectra than in the SBR gum sample. Additional two quite strong bands are also evident in the region, at 1540 and 1725 cm^{-1}, which do not belong to SBR. The more intense band (1540 cm^{-1}) is present in all the samples, and it can be ascribed to the symmetric carboxylate stretching band of zinc stearate compound.[28] The less intense band (1725 cm^{-1}) is stronger in the composites spectra than in the gum matrix. Although weakly perturbed, it can be ascribed to the C=O stretching vibration of stearic acid (1703 cm^{-1})[29].

The appearance of an additional peak (870 cm^{-1}) in the lower wavelength region of the IR spectra at higher MWCNT loading may indicate that some new specie has been formed or that some ingredient of the SBR vulcanization formulation, which normally disappears during the reactive process, has not completed its conversion. Examples for the latter are the stearic acid and its reaction product with zinc oxide, the zinc stearate, both used in excess. The TBBS accelerator is normally formulated for its complete conversion; it is dissociated into mercaptobenzothiazole (MBT) and *t*-butylamine radicals by heating at the beginning of vulcanization.[30] The MBT quickly converted into 2-mercaptobenzothiazole-disulphide (MBTS) which reactions with the rubber chains forming a crosslink precursor and leaving behind a MBT molecule. When zinc or equivalently ZnO is present as an activator in the vulcanisation system, it catalyses the sulphur insertion into the MBTS increasing the amount of sulphur atoms embedded in the crosslink precursor. Then, MBT from TBBS is a residue after vulcanization has terminated. The FTIR strong absorption band of MBT in the lower wavelength region is localized at 752 cm^{-1},[31] this band is also present in the FTIR spectra of TBBS[32] and SBR. However, there is a medium intense band at 910 cm^{-1} present in the FTIR spectra of TBBS but not in MBT, which may be assigned to S—N stretching vibration.[33] As already shown, the vibrational spectra of adsorbed dibenzothiophene (DBT) aromatic molecules on carbon nanotube support are very slightly perturbed (in band frequencies) suggesting that such molecules stands flat on the MWCNTs surface.[34] If the TBBS aromatic molecules are adsorbed like DBT molecules on carbon nanotube surface, then the band at 910 cm^{-1} could be shifted to 870 cm^{-1}, and this fact also may explain that TBBS molecules were no dissociated by heating at the beginning of vulcanization.

It has already been reported that nanotubes may act as scavengers of oxygen-centered and carbon-centered free radicals, thanks to the high electron affinity of the carbon framework.[35,36] Then, the vulcanization reaction could be also affected if the MWCNTs act as scavengers of benzothiazole radicals that form from the scissions of the S—N bond in the TBBS. These radicals could react with carboxylic and OH groups formed onto the MWCNT surface by a previous oxidation process.[37] However, the MWCNTs used in this work were not exposed to any previous treatment of oxidation; they have only a low density of reactive sites.

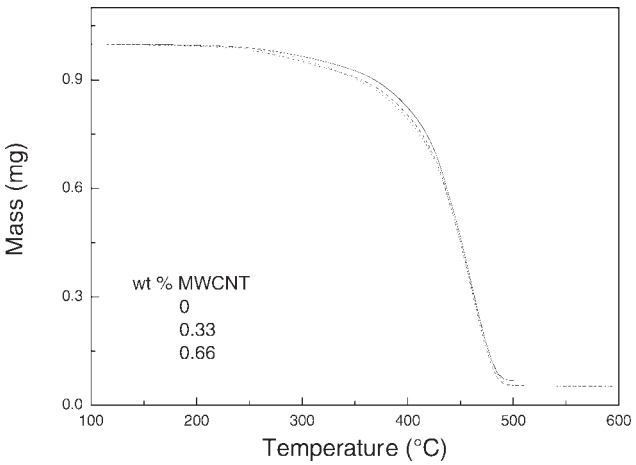

Figure 7 TGA weight loss curves SBR/MWCNT composites containing different MWCNT contents.

Thermogravimetric analysis, shown in Figure 7, was performed to study the thermal degradation of the matrix and the composites. It should be noted that the addition of MWCNT does not change the thermal degradation of the composites, compared with that of the matrix. This agrees with a previous study about flammability properties of polymer composites,[38] and it has also been observed in epoxy nanocomposites,[39] where an increased content of CNT did not change the TGA curve.

After assembling all our partial discussions, it can be concluded that a small portion of TBBS molecules is absorbed onto the MWCNT surface during the mixing process,[40] and these molecules are not dissociated into MBT and *t*-butylamine radicals by heating at the beginning of vulcanization. When the reinforcement is increased, the amount of inhibited accelerator grows as well as the sulfur/accelerator ratio, more polysulfidic crosslinks begin to appear and the maximum torque in the gum matrix decreases.[16] A special attention has to be put on the behavior of the scorch delay; there are experimental evidences with TBBS accelerator showing that the scorch time decreases as the accelerator concentration does.[41] Of course, the behavior of the total heat, rate, and order of the reaction reflect the diminution of the accelerator in the gum mixtures.

CONCLUSIONS

MWCNT provide an appreciable level of reinforcement (by weight) to a SBR rubber matrix. The experimental evidence suggests that this is due to the high aspect ratio, and good dispersion and phase adhesion of the polymer chains to the walls of the nanotubes. However, this improvement is less than expected at high filler content. This effect was attributed to a less crosslinked matrix as consequence of the adsorption of the accelerator, employed in the vulcanization, onto MWCNT surface.

A future research could be to employ accelerants without aromatic rings in their molecular structures. In particular, we proposed to use tetramethylthiuram disulfide (TMTD) or tetramethylthiuram monosulfide (TMTM) to test how is their influence on the scorch time related to the presence of nanotubes.

We thank the following institutions for their financial support: Universidad de Buenos Aires (UBACYT X-808 and X-191); Consejo Nacional de Investigaciones Científicas y Técnicas - Argentina (PIP No. 5959); Agencia Nacional de Promoción Científica y Tecnológica - Argentina (PICT No. 10-25834); Gobierno Vasco/Eusko Jaurlaritza (IE05-146 and IT-365-07 projects) and Ministerio de Educación y Ciencia/Feder (MAT2006-06331 project), Spain.

References

1. Frogley, M. D.; Ravich, D.; Wagner, H. D. Compos Sci Technol 2003, 63, 1647.
2. Kueseng, K.; Jacob, K. I. Eur Polym J 2006, 42, 220.
3. Fakhre'l-Razi, A.; Atieh, M. A.; Girun, N.; Chuah, T. G.; El-Sadig, M.; Biak, D. R. A. Compos Struct 2006, 75, 496.
4. Szleifer, I.; Yerushalmi-Rozen, R. Polymer 2005, 46, 7803.
5. Zhou, X.; Zhu, Y.; Liang, J. Mater Res Bull 2007, 42, 456.
6. Zhou, X.; Zhu, Y.; Gong, Q.; Liang, J. Mater Lett 2006, 60, 3769.
7. De Falco, A.; Goyanes, S.; Rubiolo, G. H.; Mondragon, I.; Marzocca, A. J. Appl Surf Sci 2007, 254, 262.
8. Girun, N.; Ahmadun, F.; Rashid, S. A.; Atieh, M. A. Fullerenes, Nanotubes Carbon Nanostruct 2007, 15, 207.
9. Coran, A. Y. Science & Technology of Rubber, Mark, J. E.; Erman, B.; Eirich, F. R., Eds. Academic Press: San Diego, 1994; Chapter 7.
10. Harris, J. O.; Trivette, C. D. Vulcanization of Elastomers, Alliger, G.; Sjothun, I. J., Eds. Robert E. Krieger Publishing Company: Huntington, 1978; Chapter 5.
11. Coran, A. Y. J Appl Polym Sci 2003, 47, 24.
12. Goyanes, S.; Rubiolo, G. H.; Salazar, A.; Jimeno, A.; Corcuera, M. A.; Mondragón, I. Diamond Relat Mater 2006, 16, 412.
13. Porter, M. Rubber Chem Technol 1967, 40, 866.
14. Flory, P. J.; Rehner, J. J Chem Phys 1943, 11, 512.
15. Flory, P. J.; Rehner, J. J Chem Phys 1943, 11, 521.
16. Lide, D. R., Ed. CRC Handbook of Chemistry and Physics, 78th ed.; CRC Press: New York, 1997; pp 3–55.
17. Deng, J. S.; Isayev, I. Rubber Chem Technol 1991, 64, 296.
18. Yue, D.; Zhang, L.; Liu, Y.; Shen, Z. J Mater Sci 2006, 41, 2541.
19. Kamal, H. R.; Sourour, S. Polym Eng Sci 1973, 13, 59.
20. Goyanes, S.; Marzocca, A. J. J Appl Polym Sci 2004, 91, 2601.
21. Mansilla, M.; Marzocca, A. J. J Appl Polym Sci 2007, 103, 1105.
22. Ding, R.; Leonov, A. I. J Appl Polym Sci 1996, 61, 455.
23. Nielsen, L. E.; Landel, R. F. Mechanical Properties of Polymers and Composites, 2nd ed.; Marcel Dekker: New York, 1994.
24. Gronski, W.; Hoffmann, V.; Simon, G.; Wutzler, A.; Straube, E. Rubber Chem Technol 1991, 65, 63.
25. Fernandez-Berridi, M. J.; Gonzalez, N.; Mugica, A.; Bernicot, C. Thermochim Acta 2006, 444, 65.
26. Gunasekaran, S.; Natarajan, R. K.; Kala, A. Spectrochim Acta 2007, 68, 323.
27. Shield, S. R.; Ghebremeskel, G. N. J Appl Polym Sci 2003, 88, 1653.
28. Sakai, H.; Umemura, J. Colloid Polym Sci 2002, 280, 316.
29. Xiong, C.; Zhou, Z.; Xu, W.; Hu, H.; Zhang, Y.; Dong, L. Carbon 2005, 43, 1788.
30. Gradwell, M. H. S.; McGill, W. J. J Appl Polym Sci 1994, 51, 177.
31. Rai, A. K.; Singh, R.; Singh, K. N.; Sing, V. B. Spectrochim Acta 2006, 63, 483.
32. Coblentz Society Inc. In NIST Chemistry WebBook; Linstrom, P. J.; Mallard, W. G., Eds. National Institute of Standards and Technology: Gaithersburg,MD, June 2005; NIST Standard Reference Database Number 69. Available at: http://webbook.nist.gov
33. Tanaka, Y.; Tanaka, Y. Chem Pharm Bull 1965, 13, 399.
34. Shang, H.; Liu, C.; Wei, F. J of Nat Gas Chem 2004, 13, 95.
35. Krusic, P. J.; Wasserman, E.; Keizer, P. N.; Morton, J. R.; Preston, K. F. Science 1991, 254, 1183.
36. Fenoglio, I.; Tomatis, M.; Lison, D.; Muller, J.; Fonseca, A.; Nagy, J. B.; Fubini, B. Free Radic Biol Med 2006, 40, 1227.
37. Escobar, M.; Goyanes, S.; Corcuera, M. A.; Eceiza, A.; Mondragon, I.; Rubiolo, G. H.; Candal, R. J. J Nanosci Nanotechnol 2008, in press.
38. Kashiwagi, T.; Du, F.; Winey, K. I.; Groth, K. M.; Shields, J. R.; Bellayer, S. P.; Kim, H.; Douglas, J. F. Polymer 2005, 46, 471.
39. Zhou, Y.; Pervin, F.; Lewis, L.; Jeelani, S. Mater Sci Eng A 2007, 452, 657.
40. Tournus, F.; Charlier, J. C. Phys Rev B 2005, 71, 165421.
41. Sadequl, A. M.; Ishiaku, U. S.; Ismail, H.; Poh, B. T. Eur Polym J 1998, 34, 51.